

# Multi-functional organic corrosion inhibitor

Charles K. Nmai \*

*Master Builders, Inc., 23700 Chagrin Boulevard, Cleveland, OH 44122, USA*

---

## Abstract

In this paper, the multi-functional benefits of the water-based organic corrosion inhibitor are presented and discussed, with regard to the corrosion protection of embedded steel and resistance to chemical attack; specifically, the resistance of concrete to sulfate attack and deterioration due to sulfuric acid exposure. The organic corrosion inhibitor consists of amines and fatty-acid esters and the mechanisms by which it functions are presented and substantiated. In addition to a 30% of calcium nitrite inhibitor, this amine-ester based organic corrosion inhibitor is a commonly used corrosion inhibitor in new construction. Time-to-corrosion evaluations in 0.50 and 0.40 water-cementitious materials ratio concretes of moderate and high quality show that the inhibitor was effective regardless of concrete quality, and significantly reduced chloride ingress. The permeability-reducing property of the amine-ester based organic corrosion inhibitor has also shown effectiveness in reducing deterioration due to the ingress of other aggressive species such as sulfate and sulfuric acid. For comparison purposes, the corrosion-inhibiting performance of the amine-ester based organic inhibitor is compared to that of calcium nitrite, while its effect in mitigating sulfate attack and reducing deterioration due to sulfuric acid exposure is compared to that of silica fume.

© 2003 Published by Elsevier Science Ltd.

*Keywords:* Corrosion; Corrosion inhibitor; Water-based; Organic

---

## 1. Introduction

Durability-based designs are gaining acceptance as design engineers continue to seek ways of extending the useful service lives of reinforced and prestressed concrete structures in aggressive environments. The durability issues of concern include corrosion, sulfate resistance, alkali-aggregate reactivity, and shrinkage. To meet the demands of the concrete construction industry, manufacturers of construction materials have developed and introduced speciality chemical admixtures, including corrosion inhibitors that can be used to produce the high-performance concretes required for these environments.

Of the corrosion-inhibiting admixture technologies for reinforced and prestressed concrete currently available in the marketplace, [1–6] the two most commonly used chemistries are calcium nitrite [1,2] and a water-based organic inhibitor, [3,4] which consists primarily of amines and fatty-acid esters. Calcium nitrite inhibits

corrosion by reacting with ferrous ions to form a protective ferric oxide film, [1,2] but the water-based organic inhibitor functions via a twofold mechanism; [3,4] first, by reducing chloride ion ingress into concrete through a hydrophobic property imparted by the fatty-acid esters and, second, through the formation of a synergistic protective coating on the surface of the embedded steel by the film-forming amine components as well as the fatty-acid esters. The water-based organic inhibitor also provides benefit in reducing deterioration due to the ingress of other aggressive species such as sulfate, because of its permeability-reducing property.

In this paper, the multi-functional benefits of the water-based organic inhibitor are presented and discussed, with regard to the corrosion protection of embedded steel and resistance to chemical attack; specifically, the resistance of concrete to sulfate attack and deterioration due to sulfuric acid exposure. For comparison purposes, the corrosion-inhibiting performance of the water-based organic inhibitor is compared to that of calcium nitrite, while its effect in mitigating sulfate attack and reducing deterioration due to sulfuric acid exposure is compared to that of silica fume.

---

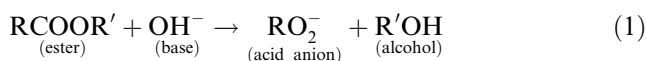
\* Tel.: +1-216-839-7302; fax: +1-216-839-8825.

E-mail address: [charles.nmai@degussa.com](mailto:charles.nmai@degussa.com) (C.K. Nmai).

## 2. Protection mechanism of multi-functional organic inhibitor

As mentioned earlier, the multi-functional water-based organic inhibitor (MFOI) inhibits the corrosion of steel in concrete by a twofold mechanism that involves the formation of a protective film on the steel surface and a reduction in the susceptibility of concrete to chloride ion penetration, or simply stated, by “chloride screening”.

When the MFOI is first added to concrete, the esters become hydrolyzed by the alkaline mix water to form the carboxylic acid and its corresponding alcohol. This reaction, under alkaline conditions, is favorable and is not easily reversed [7]. The reaction proceeds as shown in Eq. (1), where R and R' represent different hydrocarbon molecules:



The carboxylic anion is quickly converted in concrete to the insoluble calcium salt of the fatty acid [7]. The created fatty acids and their calcium salts provide a hydrophobic coating within the pores. This causes a reversed angle of contact in which the surface tension forces now push water out of the pore instead of into the pore [8]. The diameter reduction of the pore, induced from the hydrophobic calcium salt lining, also reduces aqueous species migration through the capillary pore matrix. Because the admixture is uniformly distributed throughout the concrete mixture during the mixing operation it, becomes a part of the paste fraction and its hydrophobic property is imparted throughout the matrix. This provides passive corrosion inhibition by increasing the time needed for chlorides to build up to the critical threshold level at the surface of the steel reinforcement.

After the concrete mixture is placed, key components of the MFOI are adsorbed onto the surface of the reinforcing steel to form a protective film. Simplistically, the film-forming amine component, FFA, bonds with the steel and the fatty-acid esters chain over the non-polar tails to form a tight mesh that restricts moisture, chloride and oxygen availability at the steel surface. Hence, the MFOI functions as a mixed inhibitor, affecting the anodic reaction by raising the chloride threshold for corrosion initiation and the cathodic corrosion reaction by restricting moisture and oxygen availability.

The film-forming mechanism by which the MFOI inhibits corrosion is the same mechanism by which other organic corrosion inhibitors function, that is, by adsorption on the metal surface. It is generally accepted that organic corrosion inhibitors bond to metals by adsorption, which can be physical and/or chemical in nature, due to the polar or weakly-polar characteristic

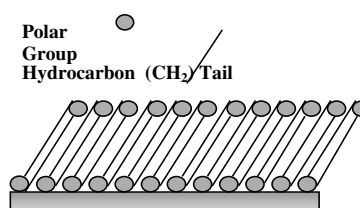


Fig. 1. FFA adsorption on steel surface.

of the organic compounds typically used in their formulation (Fig. 1). The following excerpt from “CORROSION INHIBITORS”, edited by Nathan, [9] gives a basic understanding of organic corrosion inhibitor or filming inhibitor technology:

“The mechanism by which all materials function is the same and requires their adsorption onto the metal through their polar group or head. The non-polar tail of the inhibitor molecule is oriented in a direction generally vertical to the metal surface. It is believed that the hydrocarbon tails mesh with each other in a sort of ‘zipper’ effect to form a tight film which repels aqueous fluids, establishing a barrier to the chemical and electrochemical attack of fluids on the base metal. A secondary effect is the physical sorption of hydrocarbon molecules from the process fluids by the hydrocarbon tails of the adsorbed inhibitor molecules. This increases both the thickness and effectiveness of the hydrophobic barrier to corrosion.”

The film-forming amine component, FFA, in the MFOI can be described most effectively as a surface-active chelant [10,11]. By definition, surface-active chelants are both surfactants and chelants [12,13] and their use as corrosion inhibitors is not new [14]. It is theorized that proper combination of surface-active and chelating groups in the same molecule will enable surface-active chelants to seek out the metal–water interface, undergo chemisorption with surface metal atoms or ions, and provide an insoluble adherent, protective chelate film on the metal surface. It has been well documented that chelates enhance and strengthen the chemisorption of known inhibitors through the formation of stable five- and six-membered chelate rings [15]. These rings are formed as a result of the bonding between two or more functional groups from the inhibitor (such as  $-\text{NH}_2$ ,  $-\text{OH}$ ,  $-\text{SH}$ ,  $-\text{COOH}$  and  $-\text{SO}_3\text{H}$ ) [14] and the cation metal as seen in the sarcosine-type surface chelate in Fig. 2.

When the FFA is chemisorbed onto the steel surface it is resonance stabilized by delocalization of the electrons through the formation of a stable six-membered ring. Corrosion research has indicated that surface chelation provides enhancement of already existent

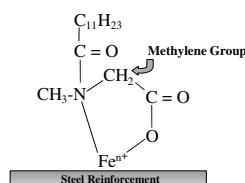


Fig. 2. Sarcosine-type surface chelate.

corrosion inhibition properties and that surface-active chelants possessing large hydrophobic substituent groups promote adsorption onto the steel surface [14] and once adsorbed improve the hydrophobic barrier to electrolyte penetration [16]. In addition, this barrier may be enhanced by the ability of the hydrophobic tails of the chelated FFA to attract other hydrocarbon molecules, such as additional FFA molecules or the waterproofing ester, to create an additional water-repellent oil film [9].

### 3. Verification of protection mechanism of multi-functional organic inhibitor

#### 3.1. Hydrophobic property

The hydrophobic or waterproofing property imparted to concrete by the fatty-acid esters in the MFOI has been demonstrated through chloride transport (flux and migration), sorption (capillary absorption) and ongoing, long-term time-to-corrosion studies.

The chloride flux, chloride migration and sorption were performed on three reference concrete mixtures and one MFOI-treated mixture using nominal cement contents of 356 kg/m<sup>3</sup> and a water-cementitious materials ratio (w/cm) of 0.45. The concretes were air-entrained. The chloride flux and chloride migration tests were performed using two-compartment cells and specimen thicknesses of 25 and 50 mm as shown in Fig. 3(a) and (b), respectively. No voltage was applied across the cells in the flux test, however, an electrical potential of 12 V was used in the migration test to saturate the specimen with a constant chloride concentration. Sorptivity was determined in accordance with the Nordtest Method NT BUILD 386, “Capillary Absorption” uti-

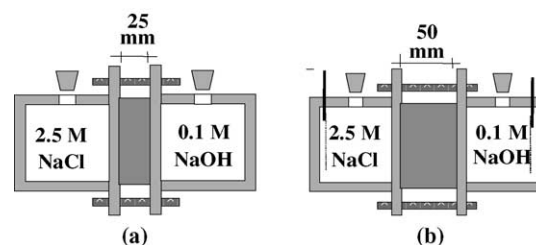


Fig. 3. Chloride flux and chloride migration test set-up: (a) chloride flux apparatus and (b) chloride migration apparatus.

lizing a 2.5 M NaCl solution. Further details of the chloride flux, chloride migration and sorptivity tests are presented in Ref. [11]. The chloride flux, chloride migration and sorptivity data are summarized in Table 1.

Diffusion coefficients from the chloride flux and chloride migration testing for the reference concretes ranged from 36–41 to 58–73 mm<sup>2</sup>/yr with averages of 39 and 64 mm<sup>2</sup>/yr, respectively. The data in Table 1 show that, relative to the reference mixtures, the MFOI reduced chloride transport by approximately 13% in the chloride flux test and by 30% in the chloride migration test. In the sorptivity tests, the average sorption rate for the MFOI-treated concrete was 3.3 g/m<sup>2</sup> s<sup>1/2</sup> compared to an average of 7.6 g/m<sup>2</sup> s<sup>1/2</sup> for the reference concretes, a reduction of 56% in capillary absorption rate.

Chloride data from an ongoing long-term corrosion evaluation of the MFOI have shown significant reductions in chloride ingress under cyclic wetting and drying conditions [17]. The amounts of acid-soluble chlorides that penetrated into the concrete specimens after 1000 and 2240 days of cyclic ponding were determined from chloride analyses of 0.375-mm thick slices cut from cores obtained from companion unreinforced specimens. The data are presented in Tables 2 and 3 and graphically in Figs. 4 and 5, respectively, for the two test ages. The Mixture ID used in the tables and figures represent the treatment, water-cement ratio (w/c) and the inhibitor dosage in liters for the inhibitor-treated concretes.

The 1000-day data show that the chloride front has penetrated beyond the 70-mm depth in all the 0.50 w/c concretes and, at least, to a depth of 50-mm in the REF-0.4-0 and CNI-0.4-20 concretes. The chloride front

Table 1  
Chloride flux, chloride migration and capillary absorption data

Mixture	Chloride flux <sup>a</sup> (mm <sup>2</sup> /y)	Chloride migration <sup>b</sup> (mm <sup>2</sup> /y)	Capillary absorption <sup>a</sup> (g/m <sup>2</sup> s <sup>1/2</sup> )
Reference 1	41	73	8.8
Reference 2	40	60	7.4
Reference 3	36	58	6.6
<b>Reference average</b>	<b>39</b>	<b>64</b>	<b>7.6</b>
<b>MFOI</b>	<b>34</b>	<b>42</b>	<b>3.3</b>

<sup>a</sup> Average of two specimens

<sup>b</sup> Average of three specimens.

Table 2  
Chloride contents after 1000 days of cyclic ponding [17]

Mixture ID	Acid-soluble chloride content (percent by mass of concrete)/Depth from ponding surface (mm)			
	13	32	50	70
REF-0.5-0	0.983	0.746	0.719	0.566
CNI-0.5-20	1.012	0.814	0.625	0.573
MFOI-0.5-5	0.556	0.172	0.023	0.017
REF-0.4-0	0.607	0.290	0.033	<0.007
CNI-0.4-20	0.609	0.195	0.011	<0.007
MFOI-0.4-5	0.390	0.103	<0.007	<0.007

REF=reference concrete; CNI=calcium nitrite inhibitor-treated concrete.

Table 3  
Chloride contents after 2240 days of cyclic ponding

Mixture ID	Acid-soluble chloride content (percent by mass of concrete)/Depth from ponding surface (mm)				
	3	13	25	75	125
REF-0.4-0	—	—	—	—	—
CNI-0.4-20	1.231	0.763	0.574	0.021	0.019
MFOI-0.5-5	0.981	0.729	0.471	0.150	0.013
MFOI-0.4-5	1.037	0.557	0.363	0.023	0.010

\* Not sampled at 2240 days.

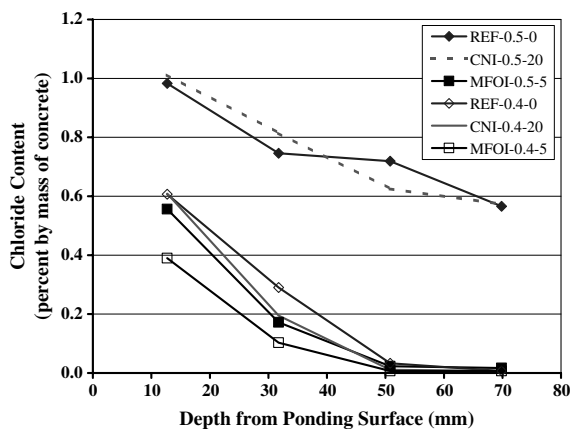


Fig. 4. Chloride content versus depth after 1000 days of cyclic ponding.

appears to be between the 32- and 50-mm depth in the MFOI-0.4-5 concrete. For the 0.40 w/c concretes, the chloride content at the 32-mm depth in the MFOI-0.4-5 concrete is 64% less than that in the REF-0.4-0 concrete and 46% less than that of the CNI-0.4-20 concrete. Furthermore, the chloride content at the same depth in the 0.50 w/c MFOI-0.5-5 concrete is 41% less than that in the REF-0.4-0 concrete and 12% less than that of the CNI-0.4-20 concrete. This strongly suggests that the MFOI at a w/c of 0.50 is more effective than 0.40 w/c concrete without inhibitor.

The 2240-day data show that, for the 0.40 w/c inhibitor-treated concretes, the chloride content at the 3, 13 and 25-mm depths in the MFOI-0.4-5 concrete are, respectively, 16%, 27% and 37% less than the corre-

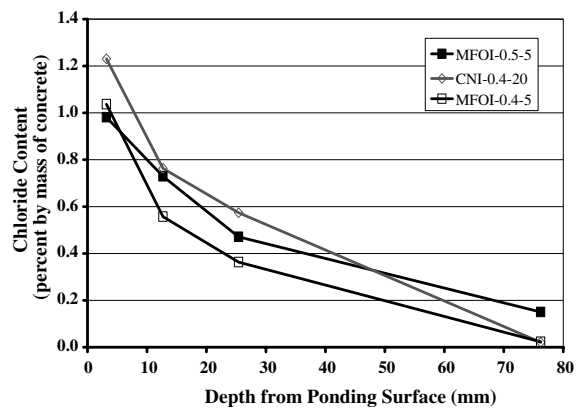


Fig. 5. Chloride content versus depth after 2240 days of cyclic ponding.

sponding chloride values in the CNI-0.4-20 concrete. Because of the long-term nature of the study, the reference specimens were not sampled at 2240 days. However, from Table 2 and Fig. 3 it can be seen that the chloride profiles for the reference concretes are quite similar to those for the 20 l/m<sup>3</sup> calcium nitrite concretes. Thus, it is reasonable to assume that their profiles at 2240 days would be similar also. This implies that similar reductions in chloride ingress can be expected between the MFOI-0.4-5 concrete and the REF-0.4-0 concrete.

Table 3 also show that the chloride content in the MFOI-0.5-5 concrete is less than that in the CNI-0.4-20 concrete at all depths, with the exception of the 75-mm depth. It can be inferred from the 2240-day data that

less chloride penetrated the MFOI-0.5-5 concrete relative to the REF-0.4-0 concrete. This is consistent with the 1000-day data and deduction, and it again suggests strongly that the MFOI at a w/c of 0.50 is more effective than 0.40 w/c concrete without inhibitor. The chloride data also show that the screening mechanism of the MFOI is still effective after 2240 days of accelerated testing, which includes three days of drying each week at 38 °C.

### 3.2. Film-forming property

Several studies have been performed specifically to verify the presence of the protective film formed by the MFOI as well as its effectiveness and impact on the rate of corrosion. These studies include Fourier transform infrared spectroscopy (FTIR), electrochemical solution tests using electrochemical impedance spectroscopy (EIS) and linear polarization (LP). The FTIR studies are presented in detail in Ref. [11] and they included a series of tests that evaluated the MFOI in mortar and saturated calcium hydroxide solution. In addition, key components of the MFOI were also evaluated in saturated calcium hydroxide solution and in various solutions including hexane and carbon tetrachloride. The following conclusions were drawn from the FTIR studies [11]:

1. Iron oxides,  $\text{Fe}_2\text{O}_3$  and  $\text{Fe}_3\text{O}_4$ , were not seen on coupons treated with the MFOI. However, different oxides were present depending upon the individual FFA and surfactant components.
2. The MFOI and its key components are strongly adsorbed onto the steel surface.
3. The FFA complexed with the steel and could not be removed from the coupons by competitive reactions with the fatty-acid ester or by solvent washing.

Verification of the effectiveness and impact of the protective film formed by the MFOI on the rate of corrosion was performed in a series of comparative electrochemical solution tests using an EG&G PAR 273-A potentiostat and an EG&G PAR 5710 lock-in amplifier. The LP procedure was performed at a potential sweep of  $\pm 20$  mV of the open circuit potential ( $E_c$ ) at a sweep rate of 0.1 mV/s. In the EIS procedure, an excitation signal with amplitude of 10 mV around  $E_c$  over a frequency range of 100 kHz to 1.5 MHz was used. The signal was applied sequentially from 100 kHz to 10 Hz using a multi-sine technique that sends a digitized waveform of prime harmonics over a range of frequencies, and then uses a fast Fourier transform to calculate the impedance for those frequencies from the cell response.

Four rounds of testing consisting of two specimens per treatment were performed using steel specimens

polished to a “600 grit” finish. In the first round of testing, only LP was performed. In subsequent rounds, each specimen was first tested by LP, allowed to depolarize for a minimum of 1 h, and then tested by EIS. At the end of each round of testing, the specimens were visually inspected for any rust deposits that may have formed. Each specimen was allowed to passivate in the test solution, saturated  $\text{Ca}(\text{OH})_2$  or saturated  $\text{Ca}(\text{OH})_2$  with the MFOI, for 4 h prior to the addition of 7.0 g of NaCl. This resulted in a test solution with a chloride concentration of 0.2 molal. The specimen was then allowed to stabilize in the chloride solution for approximately 14 h prior to testing.

Polarization resistance values from the LP test were determined using an analysis function in EG&G PARC's M352 software package and shown in Table 5. The polarization resistance was calculated by fitting a line through all points within 10 mV of the open circuit potential ( $E_{\text{corr}}$ ) of the steel coupon in the test solution, that is,  $E_{\text{corr}} \pm 10$  mV. This is in accordance with ASTM G59, “Standard Test Practice for Conduction Potentiodynamic Resistance Measurements.” Polarization resistance values from the EIS testing in Table 4 were determined by fitting the impedance data to electrical circuit models using the non-linear least squares fitting routine of the program “Equivalent Circuit” by Bernard A. Boukamp. Data from the reference was modeled using a “Randle Circuit” and the MFOI was modeled by a circuit applicable to a coated passive metal [18].

Polarization resistance ( $R_p$ ) and corrosion rate are inversely related [19]. Hence, increasing values of  $R_p$  are indicative of decreasing corrosion rates. Studies by Feliu et al. on the polarization resistance of reinforcing steel in chloride-contaminated and chloride-free concrete beams and slabs have shown that  $R_p$  values less than  $20 \text{ k}\Omega \text{ cm}^2$  are indicative of active corrosion conditions, whereas  $R_p$  values greater than  $100 \text{ k}\Omega \text{ cm}^2$  typically represent passive conditions [20]. Therefore, for the steel specimens used in this evaluation, all of which had a surface area of  $4.85 \text{ cm}^2$ , active corrosion condition was indicated by  $R_p$  values less than approximately  $4.0 \text{ k}\Omega$ , whereas  $R_p$  values greater than  $20.0 \text{ k}\Omega$  indicated passive conditions.

As shown in Table 4, the  $R_p$  data from the LP and EIS procedures were very similar.  $R_p$  values could not be determined from the impedance data for the MFOI specimens because the lowest frequency used in the EIS experimental setup was not low enough to completely examine the steel interface in this test solution. The open circuit (corrosion) potential data from the two procedures were checked before each procedure, and as indicated by the data in Table 4 they were very similar. This indicates that the 1 h depolarization period between the LP and EIS tests was sufficient and that the LP procedure was non-destructive.

The data shown in Table 4 show that MFOI had average  $R_p$  values greater than  $20 \text{ k}\Omega$ . This implies that

Table 4  
Polarization resistance and open circuit corrosion potential data

No.	Polarization resistance, $R_p$ (k $\Omega$ )				Corrosion potential, $E_{\text{corr}}$ (mV vs. SCE)			
	LP		EIS		LP		EIS	
	Ref.	MFOI	Ref.	MFOI	Ref.	MFOI	Ref.	MFOI
1	–	895	–	–	–505	–214	–	–
2	1.151	742	–	–	–436	–219	–	–
3	0.912	779	0.811	**	–530	–229	–533	–226
4	2.023	775	1.577	**	–461	–222	–470	–217
5	0.769	3009*	0.766	**	–525	–225	–528	–220
6	1.090	933	1.185	**	–511	–205	–520	–198
7	1.378	7098*	1.139	**	–529	–207	–533	–201
8	1.208	5861*	1.392	**	–513	–218	–525	–211
Average	1.219	825	1.143		–501	–217	–518	–212
Standard deviation	0.406	83.7	0.317		34.4	8.4	24.1	11.0
Standard error	12.6%	5.1%	11.3%		2.6%	1.5%	1.9%	2.1%

\* Not included in statistical calculations.

\*\* EIS curves indicated extremely passive conditions ( $R_p > 500$  k $\Omega$ ).

the MFOI effectively reduced chloride-induced corrosion of the steel specimens. The average  $R_p$  value of 1.0 k $\Omega$  for the reference specimens strongly suggest active corrosion conditions, as supported by the corrosion potential data. Visual inspection of the steel specimens also confirmed the presence of corrosion products on the reference specimens and nothing on the MFOI-treated specimens. This showed that the protective film formed by the MFOI at the surface of the steel provides active inhibition by reducing the rate of corrosion in the presence of chlorides.

#### 4. Results of time-to-corrosion evaluations of multifunctional organic inhibitor

The effectiveness of the MFOI has been demonstrated in several accelerated time-to-corrosion evaluations of the inhibitor [3,4,17] that include a long-term evaluation of untreated and inhibitor-treated air-entrained concretes containing 356 kg/m<sup>3</sup> and a low w/c of 0.40. Details of the long-term evaluation and data through 1000 days of cyclic ponding with a 15% solution of sodium chloride can be found in Ref. [17].

Macrocell corrosion current data through 1550 days of cyclic ponding are as shown in Fig. 6. The data show virtually no corrosion activity in the MFOI test specimens. The macrocell corrosion current data is supported by the half-cell potential data shown in Fig. 7, which shows half-cell potentials more positive than –200 mV CSE for the MFOI. The MFOI was used at its recommended dosage of 5 l/m<sup>3</sup>. By contrast, the control untreated specimens exhibited signs of corrosion activity after about 200 days and specimens containing 20 l/m<sup>3</sup> of a calcium nitrite inhibitor (CNI) started corroding

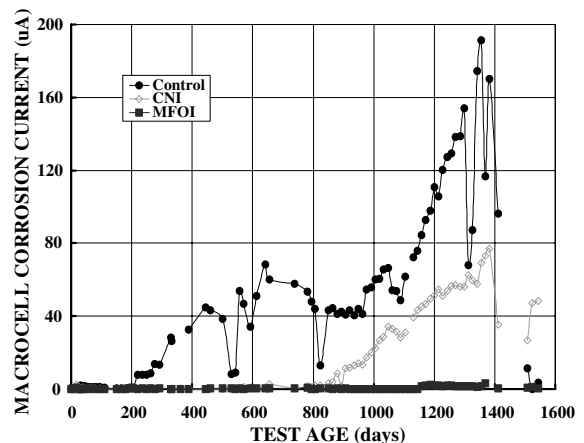


Fig. 6. Macrocell corrosion current data from comparative long-term accelerated corrosion investigation.

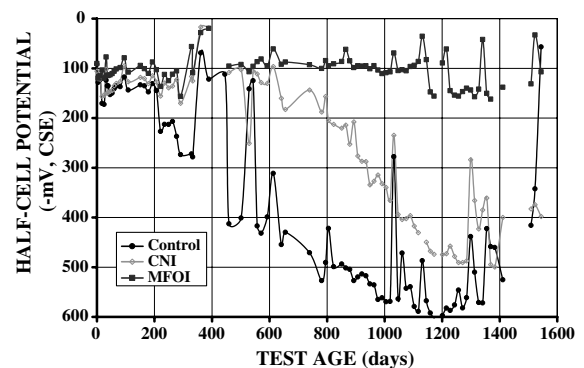


Fig. 7. Half-cell potential data from comparative long-term accelerated corrosion investigation.

## 5. Additional benefits of the multi-functional organic inhibitor

The beneficial effect of the MFOI in reducing expansion due to sulfate exposure has also been reported by Amey et al. [23] from studies that were per-

As mentioned earlier, the introduction of the MFOI into concrete results in the formation of insoluble calcium salts of the fatty acid and a hydrophobic coating within the pores. This causes a reversed angle of contact in which the surface tension forces now push water out of the pore instead of into the pore [8]. The diameter reduction of the pore, induced from the hydrophobic calcium salt lining, also reduces aqueous species

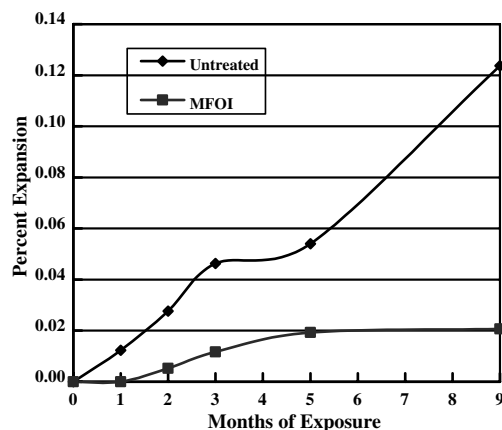


Fig. 8. Length change (expansion) due to sulfate exposure.

Table 5

Summary of concrete mixtures for sulfate and sulfuric acid exposure studies [23]

	Magnesium sulfate exposure				Sulfuric acid exposure (pH of 1)			
	Ref 1	MFOI 1	Ref 2	MFOI 2	Ref 1'	Ref 2'	MFOI 1'	MFOI 2'
Cement (kg/m <sup>3</sup> )	403	403	386	386	390	359	390	390
Silica fume (kg/m <sup>3</sup> )	24	24	—	—	—	31	—	—
Fly ash (kg/m <sup>3</sup> )	47	47	—	—	—	—	—	—
MFOI (l/m <sup>3</sup> )	—	5	—	5	—	—	2.5	5
w/cm	0.32	0.33	0.40	0.40	0.38	0.38	0.38	0.38

migration through the capillary pore matrix. The beneficial effect of the MFOI in the sulfate and sulfuric acid exposure studies may be explained by a couple of factors. First, it is likely that the solutions could not readily penetrate the concrete matrix because of the reduction in permeability imparted by the MFOI. Second, the lining of the pores by the hydrophobic coating may also reduce accessibility of the aggressive solutions to the hydrated cement paste, thus reducing the rate of reaction and overall degradation.

## 6. Effect of the multi-functional organic inhibitor on fresh and hardened properties

As reported elsewhere, [3] the MFOI has no significant impact on typical fresh and hardened concrete properties. It has no effect on water demand but, because of the fatty-acid esters, higher than normal dosages of air-entraining admixture may be required to achieve the desired air content. Unlike calcium nitrite that accelerates concrete set, the MFOI has no effect on the setting characteristics of concrete.

With regard to hardened properties other than those already discussed, a decrease in compressive strength may be experienced with the MFOI depending on the mixture ingredients. The decrease may be about 5–7.5% relative to a control untreated mixture [3]. However, because of the low w/cm required for corrosion control purposes, the strength decrease is often negligible from a design perspective for most cast-in-place construction and has not been an issue in field applications.

## 7. Summary

In this paper, the mechanism and MFOI that consists of amines and fatty-acid esters have been presented and discussed. The primary use of the MFOI is the corrosion protection of embedded steel and time-to-corrosion evaluations in 0.50 and 0.40 water-cementitious materials ratio concretes of moderate and high quality have showed that the inhibitor is effective regardless of concrete quality, and significantly reduces chloride ingress. The chloride data show that the addition of 5 l/m<sup>3</sup> of

the MFOI to 0.50 w/c concrete was more effective than lowering the w/c of untreated concrete from 0.50 to 0.40.

The permeability-reducing property of the MFOI has also shown effectiveness in reducing deterioration due to the ingress of other aggressive species such as sulfate and sulfuric acid. For comparison purposes, the corrosion-inhibiting performance of the MFOI was compared to that of calcium nitrite, while its effect in mitigating sulfate attack and reducing deterioration due to sulfuric acid exposure was compared to that of silica fume.

## References

- [1] Rosenberg AM, Gaidis JM, Kossivas TG, Previte RW. A corrosion inhibitor formulated with calcium nitrite for use in reinforcing concrete. In: Chloride corrosion of steel in concrete, ASTM STP 629. West Conshohocken, PA: American Society for Testing and Materials; 1977. p. 89–99.
- [2] Berke NS, Rosenberg A. Technical review of calcium nitrite corrosion inhibitor in concrete. In: Concrete bridge design and maintenance: Steel corrosion in concrete, Transportation Research Record 1211. Washington DC: Transportation Research Board; 1989. p. 18–27.
- [3] Nmai CK, Farrington SA, Bobrowski GS. Organic-based corrosion-inhibiting admixture for reinforced concrete. Concrete International, American Concrete Institute, vol. 14, no. 4, April 1992, pp. 45–51.
- [4] Nmai CK, Krauss PD. Comparative evaluation of corrosion-inhibiting chemical admixtures for reinforced concrete. SP-145, Proceedings of the Third CANMET/ACI International Conference on Durability of Concrete, Nice, France, ACI International, 1994. pp. 245–62.
- [5] Martin PJ, Miksic BA. Corrosion inhibition in reinforced cement. Canadian Patent no. 1,258,473, August 1989.
- [6] Mäder, U. A new class of corrosion inhibitors for concrete. Proceedings of the 2nd Regional Concrete Conference—Concrete Durability in the Arabian Gulf, Bahrain, 1995.
- [7] Carey FA, Sundberg RJ. Advanced organic chemistry, Part A: Structure and mechanisms. 2nd ed. New York: Plenum Press; 1984.
- [8] Ramachandran VS. Concrete admixtures handbook, properties, science, and technology. 2nd ed. Park Ridge, NJ, USA: Noyes Publications; 1995.
- [9] Nathan CC, editor. Corrosion inhibitors. National Association of Corrosion Engineers; 1973. p. 279.
- [10] Bobrowski G, Youn DJ. Corrosion inhibitors in cracked concrete: an admixture solution, Concrete 2000: Economic and durable construction through excellence. Proceedings of the International Conference, vol. 2, Infrastructure, Research, New Applications, 1993.

- [11] Buffenbarger JK, Miltenberger MA, Miller BD, Casal HL. Long-term performance of an organic corrosion inhibitor: a decade of mechanism study and its impact on concrete service life, Materials Week Conference, Germany, 2000.
- [12] Martell AE, Calvin M. Chemistry of the metal chelate compounds. Englewood Cliffs, NJ: Prentice-Hall, Inc; 1952.
- [13] Dwyer FP, Mellor DP, editors. Chelating agents and metal chelates. New York: Academic Press; 1964.
- [14] Luttringaus A. *Angewandte Chemie* 1952;64(24):661–70.
- [15] Zecher DC. *Mater Perform* 1976;15(4):33–7.
- [16] McCafferty E. Mechanisms of corrosion control by inhibitors. In: Leidheiser Jr H, editor. Corrosion control by coatings. Princeton: Science Press; 1979. p. 279–317.
- [17] Nmai CK, McDonald D. Long-term effectiveness of corrosion-inhibiting admixtures and implications on the design of durable reinforced concrete structures. Supplementary Proceedings of the RILEM International Symposium on The Role of Admixtures in High—Performance Concrete, Monterrey, Mexico, 21–26 March 1999. p. 1–17; In: Johal LS (Paul) editor. Proceedings of the PCI/FHWA/FIB International Symposium on High Performance Concrete, Orlando, Florida, 25–27 September 2000, PCI. p. 109–24.
- [18] Taylor R et al. Electrochemical impedance spectroscopy: theory, applications, and laboratory instruction. Course materials from The Center of Electrochemical Science and Engineering. Charlottesville, VA: University of Virginia; 1995.
- [19] Stern M, Geary AL. Electrochemical polarization: a theoretical analysis of the shape of polarization curves. *J Electrochem Soc* 1957;104(1):56–63.
- [20] Feliu S, Gonzalez JA, Feliu Jr S, Andrade C. Confinement of the electrical signal for in situ measurement of polarization resistance in reinforced concrete. *ACI Mater J* 1990;(September–October):457–60.
- [21] Pfeifer DW, Landgren JR, Zoob AB. Protective systems for new prestressed and substructure concrete. Report no. FHWA/RD-86/193, US Department of Transportation, Federal Highway Administration, April 1987, 126 pp.
- [22] McDonald DB, Pfeifer DW, Blake GT. The corrosion performance of inorganic-, ceramic- and metallic-clad reinforcing bars and solid metallic reinforcing bars in accelerated screening tests. Report no. FHWA- RD-96-085, Federal Highway Administration, Office of Engineering and Highway Operations R&D, McLean, VA, October 1996, 112 pp.
- [23] Amey SL, Buffenbarger JK, Daczko JA, Johnson DA. Durability of concrete containing and ester–amine admixture exposed to sulfate and sulfuric acid Solutions. SP-173. Proceedings of the Fifth CANMET/ACI International Conference, Rome, Italy, October 1997.